Materials Advances

ROYAL SOCIETY OF CHEMISTRY

PAPER

View Article Online
View Journal | View Issue

Cite this: *Mater. Adv.*, 2023, 4, 2926

Extrusion of uniform-diameter polyetheretherketone–magnesium phosphate bio-composite filaments for 3D printing of design-specific multi-functional implants

Vijay K. Bokam,† Surendrasingh Y. Sonaye,† Phaniteja Nagaraju, Harsha P. S. Naganaboyina and Prabaha Sikder *

Polyetheretherketone (PEEK) is a high-performance polymer material for developing implants for orthopedic, spinal, cranial, maxillofacial, and dentistry applications. However, the major limitation of PEEK implants is their bioinertness, *i.e.*, their incapability to integrate with tissues. Therefore, prior efforts have always focused on developing hydroxyapatite (HA) coatings on PEEK or PEEK–HA composites. However, in this study, we engineered a highly novel bioceramic known as amorphous magnesium phosphate (AMP), which surpasses the bioactivity and biodegradation kinetics of HA. Subsequently, we incorporated AMP in PEEK to develop a unique PEEK–AMP bioactive composite in the form of uniform-diameter filaments, such that it can be used in a fused filament fabrication (FFF)-3D printing setup to develop design-specific multi-functional implants. Our results indicate that controlling extrusion parameters such as temperature gradient, screw speed, tension, and cooling rate is essential in extruding uniform-diameter filaments suitable for 3D printing. Furthermore, rheological properties confirmed the suitability of the PEEK-AMP filaments for 3D printing, and SEM revealed the uniform dispersion of the AMP particles in the PEEK matrix. Importantly, PEEK–AMP composites exhibited a yield strength of 89 MPa and Young's modulus of 3.5 GPa, confirming that AMP incorporation in PEEK does not deteriorate the inherent properties of PEEK. Moreover, we prove that 3D printing can manufacture mechanically robust PEEK–AMP structures comparable to machined ones. This comprehensive study introduces a unique and first-of-its-kind bio-composite, better than existing ones, that can be used to develop standalone bioactive multi-functional implants for reconstructive and regenerative medicine and enhance patient and surgical outcomes.

Received 14th April 2023,
Accepted 29th May 2023

DOI: 10.1039/d3ma00172e

rsc.li/materials-advances

1. Introduction

Poly-ether-ether-ketone (PEEK) is a colorless semi-crystalline thermoplastic polymer in the polyaryletherketone (PAEK) family with excellent mechanical properties. For instance, PEEK has a tensile strength of 90–100 MPa, a compressive strength of 115–120 MPa, and a bending strength of 140–150 MPa.[1] Furthermore, it has high thermal stability compared to conventional polymers, with a melting point of 343 °C, and is inert to various corrosive chemicals and fluids. Finally, it has a superior strength-to-weight ratio, and excellent wear, radiation, and creep resistance. Due to such outstanding material properties, PEEK is considered as one of the most durable high-performance thermoplastics in the polymer industry and is utilized to make parts apt for demanding applications such as shafts, seals, bearings, casings, gears, and couplers, for the automotive, aerospace, oil, and gas industries.[2]

In addition to the demanding applications, PEEK is a highly preferred material in the medical device industry. For instance, it is one of the optimum materials-of-choice for making orthopedic, maxillofacial, cranial, dental, and spinal implants.[3] It has evolved to be the preferred biomaterial because of the following reasons. First, PEEK is biocompatible and highly stable in bodily fluids. Second, PEEK implants have mechanical properties such as stiffness (3–4 GPa) close to that of the native bone (10–32 GPa), minimizing chances of stress-shielding, a common problem with metallic implants.[4] Moreover, PEEK can also be modified by incorporating other materials, such as carbon fibers, to tailor the mechanical properties (18 GPa) and make it similar to cortical bone.[5] Finally, PEEK is radiolucent, which lets surgeons easily assess new bone formation around the implant.[6,7]

However, although PEEK exhibits several approving biomaterial properties, its inherent bioinertness, *i.e.*, inability to integrate

Department of Mechanical Engineering, Cleveland State University, Cleveland, OH, USA. E-mail: p.sikder@csuohio.edu

† Both authors made equal contributions to the manuscript.

with tissues such as bone, limits PEEK medical implants from integrating with the neighboring tissues. Many approaches have been developed to address the bioinertness of PEEK. Some of the most common ones include surface functionalization, surface texturing, etching, and coating with bioactive particles. Plasma-related surface functionalization treatments such as plasma-gas treatment with oxygen, nitrogen, argon, or ammonia, and plasma ion immersion implantation are some of the most well-known techniques to functionalize the PEEK surface and improve the wettability and bioactivity.[8] Alkali etching by sodium hydroxide[9] is yet another common way to modify the PEEK implants' surface chemistry and increase their bioactivity. PEEK surfaces roughened by sandblasting[10] or laser[11] have shown notably better osseointegration than smooth PEEK implants. Previous research has also shown that sulfonation of PEEK surfaces can create a microporous architecture on the implant and increase the bioactivity of PEEK.[10,11] On the other hand, various additional bioactive materials such as gold (Au), titanium (Ti), titanium dioxide (TiO_2), and hydroxyapatite (HA) have been deposited on the surface of PEEK implants in the form of thin films or coatings using varying coating deposition techniques to make PEEK bioactive.[12]

However, most of these techniques have certain shortcomings. For instance, coatings developed on PEEK scaffolds can delaminate due to the poor coating-substrate adhesion strength[13] or get prone to wear/coating loss during impaction,[14] thus affecting the long-term durability and bioactivity of the scaffold.[15] In addition, sulfonated PEEK can retain traces of sulphuric acid, which can be highly toxic to cells.[16] Also, only increasing hydrophilicity might not be a foolproof measure to increase the integration extent with bone (*i.e.*, osseointegration); additional bioactive properties are required to enhance bone formation at the implant–bone interface.

In contrast, incorporating bioactive particles into PEEK and forming a PEEK-based composite is an efficient process for making durable bioactive PEEK implants.[12] In this regard, HA, a well-known calcium phosphate (CaP), is the most well-known bioceramic incorporated into PEEK to develop bioactive composites. However, sufficient evidence in the literature suggests that magnesium phosphates (MgPs) outperform CaPs in bioactivity and bone regeneration.[17] We have developed various kinds of MgP coatings on PEEK, proving that they outperform HA coatings.[11,18] Especially amorphous magnesium phosphate (AMP) is a novel yet promising bioactive and biodegradable material in the MgP family with outstanding osteogenic potential.[19] For instance, Nabiyouni *et al.*[20] showed that AMPs exhibit a significantly higher pre-osteoblastic cell attachment rate than HA. Elhattab *et al.*[21] incorporated AMP particles into polylactic acid (PLA) and developed 3D-printed PLA–AMP microporous composite scaffolds with high osteogenic potential. Sikder *et al.*[19] also formed PEEK–AMP composites for dental and orthopedic applications. Similarly, Dubey *et al.*[22] incorporated AMP into an extracellular matrix (ECM) hydrogel and observed that AMP-containing bio-printed scaffolds resulted in significant new dense bone formation. Notably, the presence of Mg^{2+} ions in AMP controls several important intracellular activities, stimulates bone mineral metabolism more than CaPs,[22] and can help enhance bone cell proliferation, differentiation, and mineralization compared to only Ca^{2+} ions.[18,20,23,24] In addition, AMPs exhibit sustained dissolution rates compared with amorphous CaPs, thus making them better biodegradable materials with favorable resorption kinetics.[18,23,25]

Yet another essential requirement in state-of-the-art medicine is patient-specific implants (PSIs). It has been proven that PSIs are essential because they match the defect anatomy, provide improved primary stability, avoid preimplant bone grafting procedures, and allow for enhanced tissue preservation around implants.[26–29] Also, if primary stability is optimized, PSIs can be loaded sooner, helping in fewer patient visits, better soft-tissue profiles, and quicker treatment time.[30,31] In addition, the precision fit of PSIs in defects can reduce bacterial growth by minimizing implant–bone gaps and facilitating osseointegration.[32] We attempted to fabricate PSIs using Computer Numerical Control (CNC), but it involved significant material wastage. Unlike CNC, Fused Filament Fabrication (FFF)-3D printing is a sustainable and powerful manufacturing method that utilizes constant-diameter filaments for making PSIs.[33]

Thus, in this study, we developed bioactive PEEK–AMP composite filaments using a combinatory approach involving planetary ball milling and extrusion. Controlled tension and spooling ensured that the filaments were of uniform diameter. It is challenging to extrude PEEK due to its high melt viscosity and melting point. Furthermore, adding secondary particles in PEEK can complicate the extrusion process. However, to our knowledge, no studies have provided a detailed analysis of the extrusion of uniform-diameter PEEK-based composite filaments. This study will provide a detailed analysis of the extrusion of PEEK–AMP composite filaments and the critical parameters for developing uniform-diameter filaments for 3D printing. After filament fabrication, the PEEK–AMP composite filaments were thoroughly analyzed based on the extrusion parameters. Subsequently, they were utilized in an FFF-3D printing machine to develop standard-specific parts for mechanical property analysis.

2. Materials and methods

2.1 AMP synthesis

AMP synthesis was carried out in-house, following the ethanol-assisted precipitation method[34] as developed by Sikder *et al.*[19] First, 11.52 g of magnesium nitrate hexahydrate ($Mg(NO_3)_2{\cdot}6H_2O$), 98% purity, (Fischer Scientific, Hampton, NH, USA) was added to 100 ml of water and 100 ml of ethanol (190 proof, Fischer Scientific, USA) followed by stirring. In a separate beaker, 2.97 g of diammonium hydrogen phosphate ($(NH_4)_2HPO_4$, 99% purity, Fisher Scientific, USA) was added to 250 ml water. Then, 45 ml ammonium hydroxide solution (11 M) and 295 ml ethanol were added to the latter mixture of diammonium hydrogen phosphate. Subsequently, the magnesium nitrate hexahydrate solution was added to the latter solution, resulting in a white precipitate formation. The precipitates were collected immediately, centrifuged, and washed in ethanol. Finally, the precipitates were dried overnight in a convection oven at 60 °C. Once dried, the AMP powders were milled and hand-ground in a mortar and pestle to

form fine powders. The powders were sieved through a No. 120 sieve to ensure that the particle size of the powders was approximately 80 μm.

2.2 Milling of PEEK–AMP powders

The 450G PEEK powders with a particle size of 80 μm were procured from Polyclean Technologies Inc and dried overnight before the milling procedure. 5 vol% of AMP was uniformly mixed with PEEK particles using planetary ball milling. We chose 5 vol% as we did not want to use a higher bioceramic incorporation extent and increase the chances of brittleness in the composites. First, the dried AMP and PEEK powders were mixed manually in 250 ml stainless steel vials. Then, the vials were set in a vertical high-energy planetary ball milling setup (MSE Supplies LLC, Tucson, Arizona, USA), in which the milling procedure was performed. The following parameters were used for the milling process: milling speed: 400 rpm, milling duration: 2 h, and ball-to-powder ratio: 2 : 1. Stainless steel balls with different diameters, such as 10 mm, 5 mm, and 3 mm were used as the milling medium.

2.3 Extrusion of uniform-diameter AMP–PEEK filaments

The entire setup used for developing the uniform diameter biocomposite filaments is shown in Fig. 1. First, the milled powders were dried overnight at 60 °C in an oven. Prior to the extrusion process, the barrel was purged thoroughly step-by-step, first by using a mid-temp (180–300 °C) purging material (Asaclean) at 200 °C and then by using a high-temp (280–400 °C) purging material at 280 °C. Purging is mandatory as it cleans the screw and barrel and avoids clogging during the process. After raising the barrel temperature to 380 °C the milled PEEK–AMP powders were placed in the hopper. A vibrator was placed into the hopper to allow easy passage of powders from the hopper into the extrusion barrel. Once the powders started moving into the barrel, the screw speed was first set to a higher speed of around 15 rpm to create easy flowability of the PEEK–AMP composites. The temperatures of all four heaters were adjusted in descending order (H1 > H2 > H3 > H4 = 380 °C > 375 °C > 370 °C > 360 °C) to build the pressure, which plays a vital role in extruding the high-temperature polymers. Once the composite extruded out of the nozzle, the screw speed was adjusted to 6–8 rpm to maintain uniform filament extrusion. The cooling fans were set to a 60% cooling rate. The extruded filament was conveyed through the puller wheels just placed under the nozzle. A diameter measuring sensor between the nozzle and the puller wheels was utilized to measure the diameter. Based on this measurement and the extrusion rate, the speed of the puller wheel was controlled by the setups inbuilt software; this created a controlled tension which helped in pulling the filament and ensuring a uniform diameter. Once a filament with a consistent uniform diameter (1.75 ± 0.10 mm) was achieved, the filament was passed through a positioner onto the spooler wheel mounted on the winder. Finally, once sufficient tension was built in the filament, the controlled movement of the winder was used to spool the filament.

2.4 Rheological characterization

Complex viscosity (η^*), elastic modulus (G'), and viscous modulus (G'') for PEEK and PEEK–AMP composites were determined using a rotational rheometer (ARES G2, TA Instruments, TA, USA). The filaments were pelletized and placed between the 25 mm parallel plate, and oscillatory shear tests were conducted

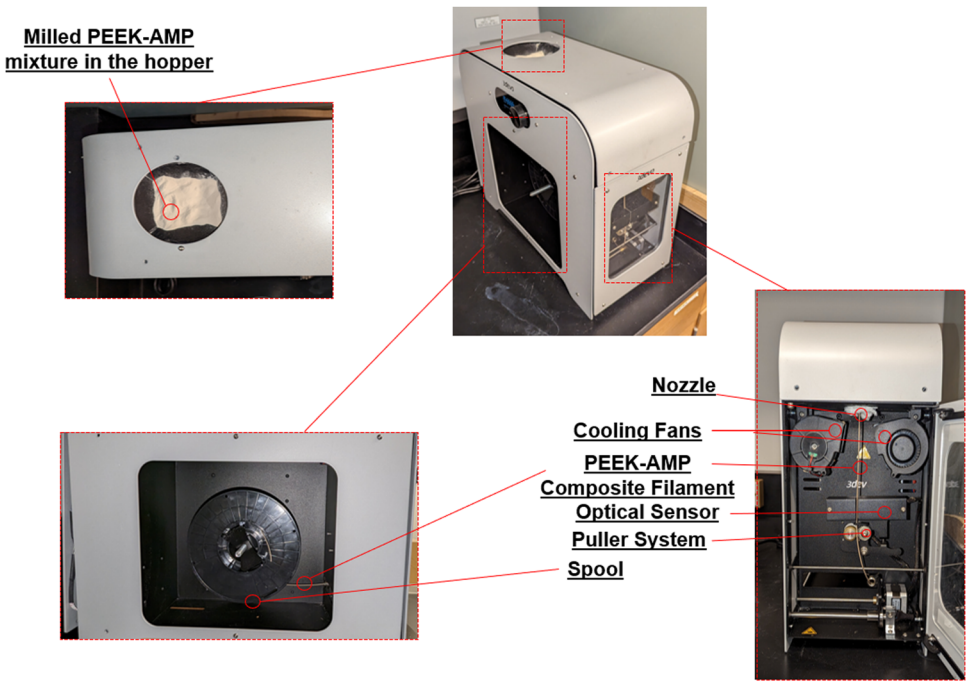

Fig. 1 Setup of the single-screw filament extruder used for forming the PEEK–AMP composite filaments.

at 370 °C, under a N_2 environment. To determine the linear viscoelastic range (LVR), *i.e.*, the region where the elastic and viscous modulus is independent of the applied strain, dynamic strain sweep tests were performed in the strain range of 0.1–100% at a constant frequency of 10 rad s^{-1}. Subsequently, the dynamic frequency sweep measurements were made using 10% strain amplitude and 0.1–500 rad s^{-1} frequency range.

2.5 Physical characterization

The structure of the extruded filament was either analyzed by digital photographs or scanning electron microscopy (SEM). The filament cross-sections and surfaces were examined using SEM with a backscattered electron diffraction (BSED) detector. Elemental analyses were carried out with energy dispersive X-ray spectroscopy (EDS, INCA, Oxford) at 20 kV and 15 mm working distance.

2.6 Thermal characterization

Approximately 10 mg of pure PEEK and the PEEK–AMP composite filaments were placed in aluminum pans for differential scanning calorimetry (DSC). The specimens were heated in the temperature range from 50 °C to 400 °C with a heating rate of 10 °C min^{-1}. Subsequently, they were cooled down to 50 °C and reheated again from 50 °C to 400 °C. The first heating cycle was performed to remove any thermal history or strains induced during the milling cycle. Specifically, data was collected from the second heating run to analyze the thermal behavior of the PEEK–AMP composites. Nitrogen at a flow rate of 50 ml min^{-1} and pressure of 5 bars was used as purging gas.

The degree of crystallinity by weight (X_{cw} (%)) was evaluated using the equation:

$$X_{cw}\ (\%) = \frac{H_m}{W_f \times H_c} \times 100$$

where H_m is the melting enthalpy obtained from the DSC scan, W_f is the weight fraction of PEEK in the composite and H_c is the melting enthalpy of fully crystallized PEEK (130 J g^{-1}).

2.7 Mechanical property analysis

The PEEK–AMP filaments were used in a FFF setup (Funmat HT Enhanced) to 3D print standard-specific parts for mechanical property analysis. For tensile testing, ISO 527-2 was followed (Fig. 2).[35] The specimen dimensions are shown in Fig. 2(i). Fig. 2(ii) shows an ongoing 3D printing of dog-bone-shaped tensile test specimens using the FUNMAT HT Enhanced with optimal parameters as shown in the Table 3 and Fig. 2(iii) shows the picture of a completed tensile test specimen. An Instron 3369 Universal Testing Machine (UTM) with a 50 kN load cell was used for the tensile tests, as shown in Fig. 2(iv). 5 mm min^{-1} strain deformation was used for measuring the strength and elongation of the specimens, and 1 mm min^{-1} strain deformation was used for measuring the modulus. Fracture surfaces of the tensile specimens were analyzed using SEM. The tensile specimens were printed at the following temperatures: 450 °C for the nozzle, 160 °C for the bedplate, 70 °C for the chamber, 0.2 mm for the layer height, and 50 mm s^{-1} for the printing speed.

2.8 Statistical analysis

All the tests were carried out in triplicates. One-way and two-way analysis of variance (ANOVA) and *post-hoc* Tukey's test were performed to analyze the data. A level of significance of $p < 0.05$ was chosen for all the statistical analyses.

3. Results and discussion

Developing filaments for 3D printing is more challenging than conventional melt extrusion, as the extruded filaments consistently need to be of uniform diameter. It becomes more complicated when high melt-viscosity polymers such as PEEK are used. Furthermore, when secondary particles are added, it can interrupt the normal flow of the polymer and make the 3D printable filament formation process more challenging. In the present study, we attempted to develop PEEK–AMP (polymer-ceramic) uniform-diameter composite filaments for the 3D printing of multi-functional implants. We observed that several parameters in the extrusion process play a significant role in developing high-quality filaments, which is essential for the FFF process.

3.1 Effect of extrusion parameters on the filaments

3.1.1 Effect of extrusion temperature on filament quality. The extrusion temperature played a major role in the flowability of the PEEK–AMP composites during extrusion. The temperature profile in the extrusion barrel helped maintain a continuous flow

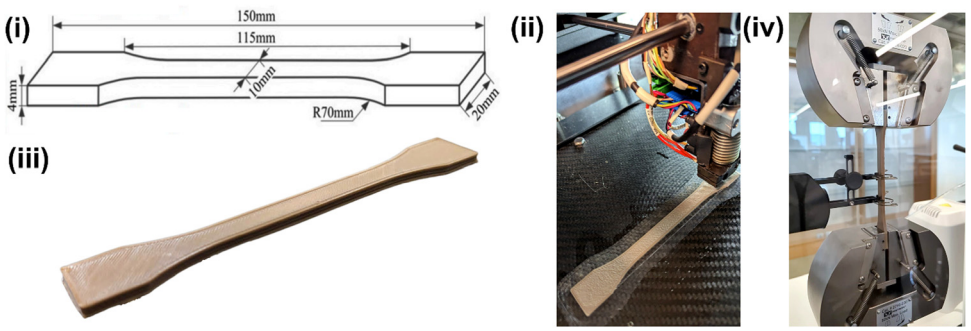

Fig. 2 Fused filament fabrication (FFF) of PEEK–AMP specimens for tensile testing. Details about the test are shown in (i) through (iv). (i) CAD drawings of the specimens. (ii) Digital photograph showing the 3D printing of the PEEK–AMP test specimens. (iii) Digital photograph of the finished PEEK–AMP test specimen. (iv) Photograph of the ongoing mechanical test.

of the PEEK–AMP melt which is essential for extruding and spooling the 3D printable filaments without interruptions. The 3devo extruder has four zone heaters: H1 = closest to the nozzle, H2 = just adjacent to H1, H3 = just adjacent to H2, and H4 = adjacent to H3 and nearest to the hopper. When all four heaters were set to 400 °C, the extruded filaments had projections of black particles on the surface, as shown in Fig. 3(a)-(i) and b-(ii). The black particles correspond to burnt polymer particles when observed closely. The exposure to the continuous high temperature inside the barrel caused the polymer particles to degrade/burn, creating projections on the filament surface, as shown in Fig. 3(b)-(ii). In addition, the filaments formed were distorted with a rough surface and hollow inner core, as shown in Fig. 3(a)-(ii) and (b)-(iii). This phenomenon is called melt fracture and causes a helical distortion on the outer layer of the filament. Melt fracture is usually observed in the filaments when the shear rate exceeds the composite flow's critical shear rate and interrupts the continuous flowability. Hu *et al.*[36] revealed the transition mechanism from a steady flow state to an unstable and discontinuous flow state with an increasing shear rate. An absorbing–releasing transition extrusion energy leads to steady–slip transition at the interface of the polymer-ceramic melt, which causes the melt fracture.

Notably, melt fracture was evident in the filaments when the temperature of all the heaters was lowered to 360 °C. At lower temperatures, such as 360 °C, the composites do not melt completely and remain in a semi-solid state exhibiting high viscosity. Especially polymers such as PEEK, which exhibit high melt viscosity, need a much higher temperature than their melting point to experience a continuous flow. Furthermore, incorporating secondary particles in the polymer matrix interrupts the

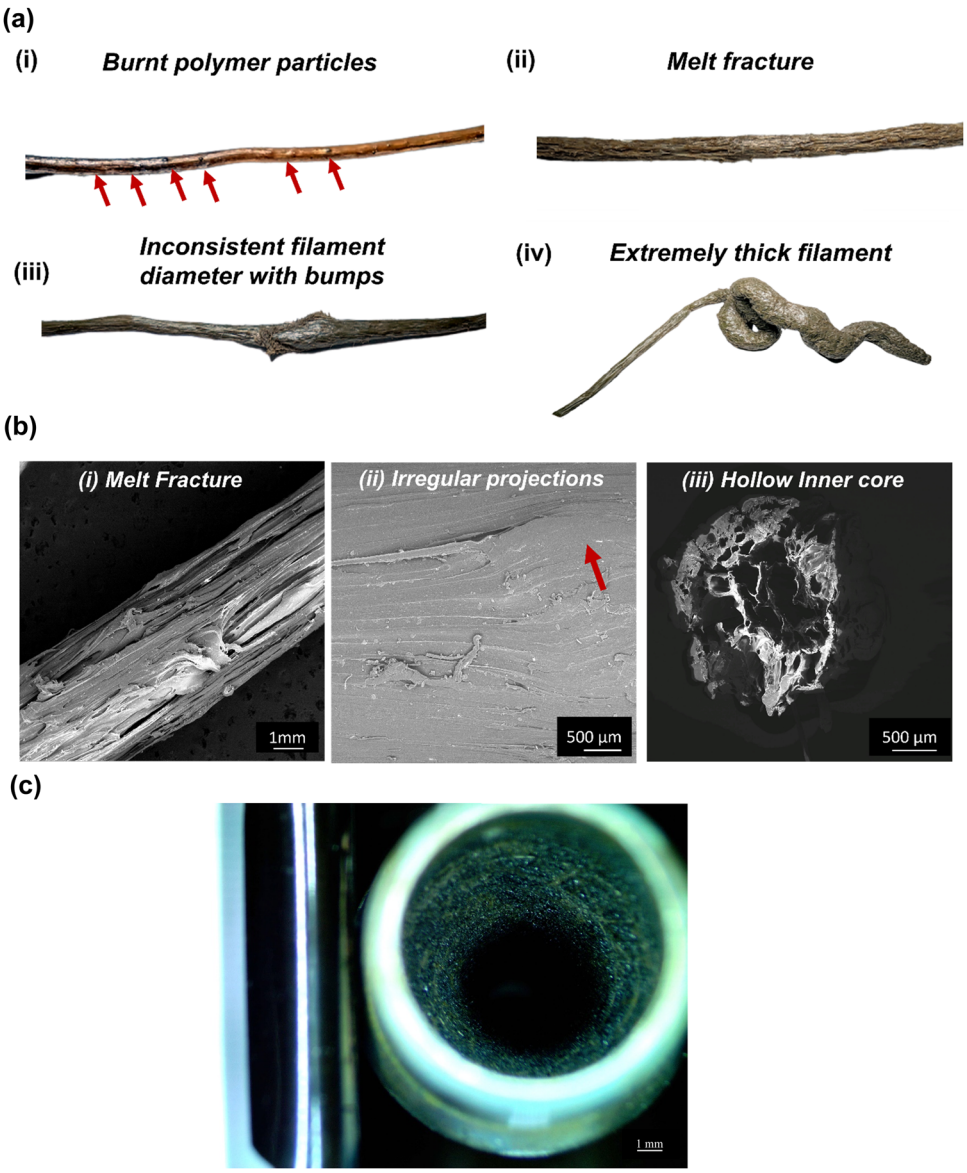

Fig. 3 (a) Digital images and (b) scanning electron microscopy (SEM) images of the filament defects due to improper extrusion. (c) A stereomicroscope image showing build-up in the interior walls of the extrusion nozzle.

continuous flow of the composite melt. Creating a pressure difference in the barrel for the composite melt to flow is essential to mitigate this issue. Hence, the temperature of H1 (the heater closest to the nozzle) was raised to 380 °C, and the remaining heaters were set in descending order, *i.e.*, H1 > H2 > H3 > H4 = 380 °C > 375 °C > 370 °C > 360 °C. The highest temperature of the heater (H1) helped the composites to be in a less viscous state, creating a zone of low pressure. As opposed, the composites in the region of H2–H4 exhibit higher viscosity than the ones in the region of H1, creating a zone of high pressure. This helps the composite melt to continuously flow from the region of higher pressure, *i.e.*, from H2–H4, to the region of lower pressure. *i.e.*, H1, forming uniform diameter filaments with smooth surface finish. However, this approach was only suitable for high-temperature polymers such as PEEK. Wang *et al.*[37] utilized the same setup but did not follow any specific ascending or descending order for the heater temperatures to extrude consistent-diameter polycaprolactone (PCL)–HA filaments. Instead, the authors maintained a high temperature for H2 and H3 for efficient mixing of the HA particles in the PCL matrix. Polycaprolactone has a much lower melting point (~65 °C) and melt viscosity than PEEK; hence it is easier to mobilize the HA particles and disperse them in the PCL matrix. In the present study, we used a mixing technique to homogeneously mix the PEEK–AMP composites before the extrusion process, as single screw extrusion will not be sufficient to disperse AMP particles homogeneously in the highly viscous PEEK matrix even if we increase the temperatures of H2 and H3. The milling process before the extrusion helped achieve a homogeneous dispersion of the AMP particles in the PEEK–AMP composite filaments. Thus, the choice of heating profiles in the extruder depends on the polymer matrix's flow and material properties and has distinct influences on forming different kinds of composite filaments.

Even though we solved the issue of melt fracture and degraded polymer, nozzle build-up was a major problem. This phenomenon happens when material remains/builds up around the exterior and interior edges of the nozzle (Fig. 3(c)); even though it is physically removed. It usually happens when the nozzle temperature is below the melting temperature of the polymer matrix. However, in the present case, even though the nozzle temperatures were higher than the melting point of PEEK, nozzle build-up was a recurrent problem. This was primarily due to two reasons. First, the ambient air around the nozzle reduced its exterior (wall) temperature and contributed to forming build-ups. For instance, the ambient atmosphere (in a cool room with temperatures of 17–20 °C) cooled down the nozzle's exterior even if it was set to 380 °C. Thus, the polymer matrix solidifies when the composite melt leaves the nozzle. Especially, this is problematic with PEEK as compared to the conventional polymers, as PEEK has higher crystallization kinetics. The build-up issue can be solved by raising the localized air/environment temperature, *i.e.*, in the region just around the nozzle with an additional external heater. In the present study, we used an external ceramic heater to raise the temperature around the nozzle to 120 °C and added extra insulation around the nozzle using kaowool, as shown in Fig. 1. This helped avoid nozzle build-ups and a continuous flow of the composite felt out of the nozzle forming filaments with a good surface finish.

3.1.2 Effect of screw speed on filament quality. Screw speed determined the extrusion rate and primarily influenced the diameter of the filaments. First, it was hypothesized that a faster screw speed would help the continuous flow of the PEEK–AMP composite melt. When the screw speed was set to 10 rpm, it formed filaments with a hollow core, as shown in Fig. 3(b)-(iii). Moreover, the filaments exhibited a highly rough surface texture, as shown in Fig. 3(a)-(ii) and (b)-(i). The high screw speed resulted in the following scenarios. First, the polymer chains did not get enough time to orient during the extrusion process, which resulted in a highly uneven surface. Second, the high screw speed did not help build up and maintain the required pressure inside the barrel, which is essential for the composite melt to exhibit a continuous flow. Instead, the high screw released the pressure inside the barrel, thus resulting in discontinuous extrusion and rough filament surfaces with a hollow core. Third, the composites did not get sufficient time to cool down as they exited the nozzle due to the high screw speed and entwined around the puller wheels. Finally, the screw speed did not provide enough time for the filament to cool down and pass through the puller wheels. Incomplete cooling kept the composite in a semi-solid state, and thus the pressure from the puller wheels flattened the semi-solid PEEK–AMP melt and failed to form the filament. When the screw speed was decreased to a slower speed, *i.e.*, 5 rpm, the filaments exhibited a good (smooth) surface finish. However, the filaments were much thicker than 1.75 mm, and bumps or excess material accumulation were observed in various regions of the filament, as shown in Fig. 3(a)-(iv) and (b)-(ii). The lower screw speed resulted in the accumulation of the PEEK–AMP composites in the barrel, increasing the pressure at the nozzle and thus creating thicker filaments (>1.75 mm) with a non-uniform diameter (unsuitable for 3D printing) [Fig. 3(a)-(iv)]. Expansion of the molten polymer or composites is the primary mechanism at lower speeds for pushing the melt to flow through the nozzle, thus increasing the filament diameter. Interestingly, this phenomenon differs from what Geng *et al.*[38] observed. The authors observed that at a lower extrusion speed, the extrusion force does not lead to swelling of the melt die, and the filament diameter is close to the nozzle diameter. In addition, the authors established a relationship that the extruded filament diameter increased with an increase in extrusion force owing to the viscoelasticity of PEEK polymers. However, it should be noted that the latter study focused on the extrusion of PEEK filaments during FFF. In general, low extrusion speeds do not create sufficient pressure drop inside the barrel, which leads to cavity formation and volume expansion due to the transition of chain disentanglement, which can increase the diameter of the extruded filaments. Lower extrusion speeds also have a higher chance of creating extrusion defects such as cavities and voids.[38]

Therefore, the extrusion rate was slightly increased and maintained at 6–8 rpm. This moderate speed helped build up an optimum pressure inside the barrel, resulting in continuous extrusion and forming the filament with a smooth surface finish.

With this increased optimum speed, the screw speed becomes a more pronounced mechanism for extruding the filaments than the free expansion of the molten polymer; hence the forced flow and the pressure drop help sustain a continuous extrusion and form the filaments with a uniform diameter. Moreover, this moderate speed provided sufficient time for the filaments to cool down, solidify and pass through the pullers without any deformation/flattening. As a result, the tension from the pullers helped form and maintain a uniform filament diameter with no deformations. As per the mechanism of the extrusion process, there must be a pressure drop in the composite melt flow throughout the liquefier. In the present case, sufficient pressure drop was created when the screw speed was carried out in the 6–8 rpm range. Fig. 4(a) shows the diameter variations in the extruded PEEK–AMP filament. The live recording during ongoing extrusion confirmed that the diameter was within acceptable tolerances over the course of the procedure. Fig. 4(b) shows a spool of the PEEK–AMP filaments with uniform diameter (1.75 ± 0.10 mm) suitable for 3D printing.

The results of the present study are similar to previous ones that dealt with the development of 3D printable filaments. For instance, Ponsar *et al.*[39] observed high degrees of diameter fluctuations *n* the extruded filaments when the screw speed was higher than 40 rpm. However, at lower screw speeds (20–40 rpm), the diameter variations were lower due to higher barrel filling degrees, and sufficient material was present to convey the melt formulation homogenously.[39] As a result, the authors achieved the least diameter variations in the filaments produced with 20 rpm and 5 g min^{-1}, much higher values than the ones in the present study.

3.1.3 Effect of cooling rate on filament quality. The cooling rate played a significant role in the crystallization of the composites and, ultimately, forming the filaments. Moreover, the cooling rate and screw speed combinedly influence the formation of uniform-diameter filaments. For instance, when the cooling and screw speed was set at 60% and 10 rpm, the filaments were flattened with the rolling action of the puller wheels. As explained earlier, this happened because the composites did not have enough time to cool down and solidify. Even though the cooling was as high as 60%, it did not get sufficient time to solidify due to

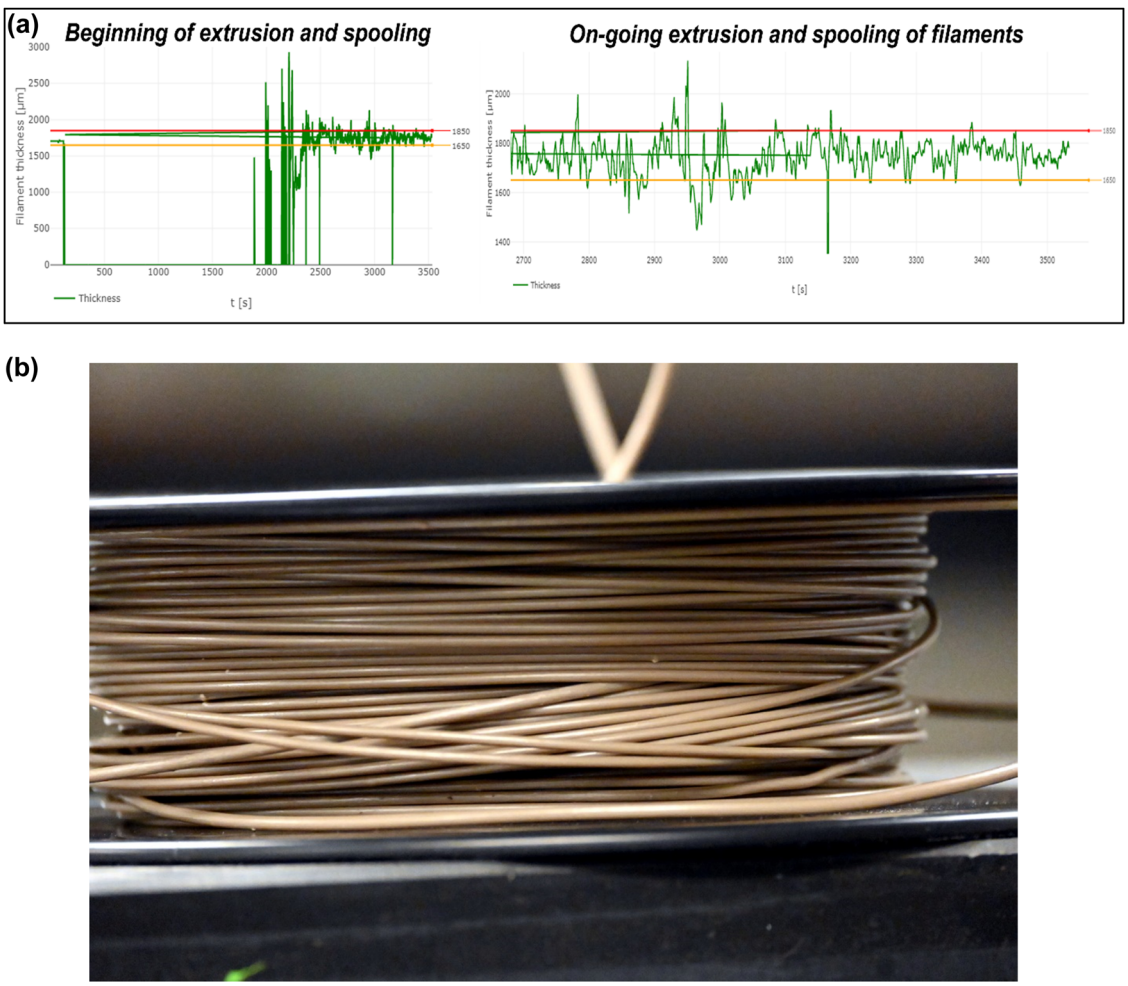

Fig. 4 (a) The variation of the filament thickness (recorded as live view) during the ongoing extrusion and spooling of the PEEK–AMP filaments. (b) A 500 gm spool of uniform-diameter PEEK–AMP composite filament (∅ 1.75 mm) developed by the 3devo setup.

the high screw speed. Moreover, it also leads to winding up around the puller wheels and solidifies, thus inhibiting the functioning of the puller wheels and the formation of uniform diameter filaments. Thus, to enhance the cool-down of composites, the cooling rate was increased to 80%, keeping the speed fixed at 10 rpm. However, the higher cooling and fast screw speed resulted in rapid and incomplete crystallization and forming thinner filaments ($<$1.75 mm). In addition, the thin filaments were tough to spool as they fractured while guided on the spool. When the screw speed was decreased to 5 rpm and the cooling rate was reduced to 40%, thick filaments ($>$1.75 mm) with non-uniform diameters were observed. Even though the composites solidified at this low cooling rate, the slow screw speed led to build-up inside the barrel, resulting in thicker filaments and excess material accumulation at various regions in the filament.

On the contrary, when the screw speed was lowered to 6–8 rpm, and the cooling rate was set at 60%, smooth surfaced filaments with uniform diameters were achieved. 60% cooling rate was optimum for solidifying the filaments, and the screw speed in the 6–8 rpm range was perfect for extruding the filaments. The solidified regions of the filaments were set into the pullers without flattening and deformation; the rotatory motion of the puller provided the pull to the extruded composites, which helped maintain the filament's uniform diameter.

However, it should be noted that in addition to the cooling rate, the temperature of the ambient atmosphere plays a major role in influencing the quality of the filaments. For instance, if the ambient temperature drops to 17–19 °C, it can cool down the air temperature around the nozzle and the cooling fans, resulting in rapid cooling down of the composites as soon as they exit the nozzle, leading to incomplete crystallization of the polymer matrix, build-ups, and discontinuous extrusion. On the contrary, if the ambient temperature is within 25–27 °C, it helps keep the air temperature around the nozzle and fans warm enough to allow the composite melt to leave the nozzle in a semi-solid state and sustain a continuous extrusion.

3.2 Rheological properties of the PEEK–AMP filaments

Polymer-based composites commonly exhibit viscoelastic behavior, which is related to its inherent molecular structure and formulation. Evaluating the relationship between molecular structure and viscoelastic behavior requires that rheological measurements be conducted in regions where the viscoelastic properties are independent of imposed strain values, *i.e.*, the LVR. Fig. 5(a) shows the results of the strain amplitude tests. For the bare PEEK sample, both G' and G'' exhibited a plateau at strain amplitudes lower than 40% and a nonlinear region at higher strain amplitudes. However, in the case of the AMP–PEEK filaments, G' and G'' increased in magnitude at low strains. Furthermore, the critical strain amplitude, γ_c, (defined as a transition point between linear and non-linear viscoelastic behavior) decreased for PEEK–AMP filaments. Notably, the results confirmed

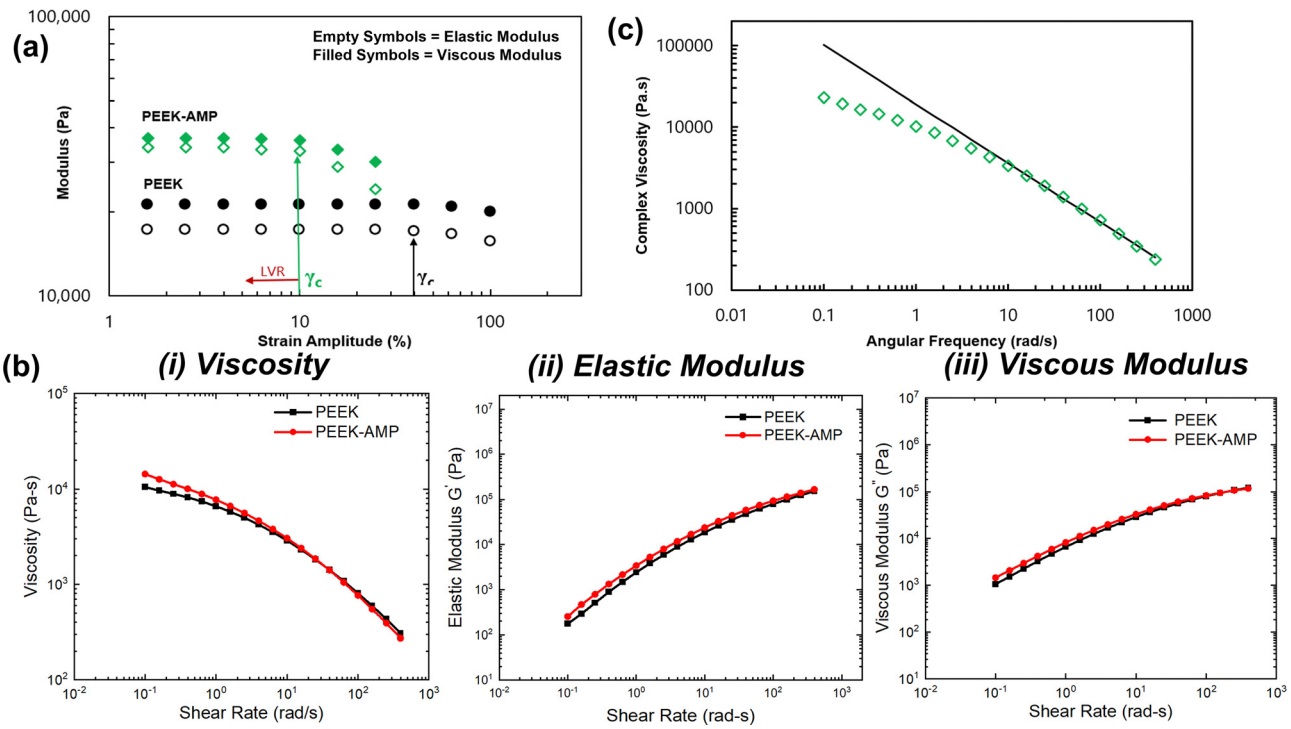

Fig. 5 Rheological properties of the PEEK–AMP composites. (a) Strain amplitude tests to determine the linear viscoelastic region (LVR) for PEEK–AMP composite filaments at 370 °C. (b) (i) Complex viscosity (η^*), (ii) elastic modulus (G'), and (iii) viscous modulus (G'') of PEEK and PEEK–AMP filaments. (c) Dynamic viscosity fitting of PEEK–AMP composite filaments (green diamond) at 370 °C with power-law model (solid line).

a LVR of less than 10% strain amplitude for the PEEK and AMP–PEEK filaments.

Fig. 5(b)-(i)–(iii) shows the rheological properties, *i.e.*, η^*, G' and G'' of PEEK and PEEK–AMP 3D printable filaments. Some interesting observations can be made. First, at lower frequencies, η^*, *i.e.*, the complex viscosity of the PEEK–AMP filaments, were higher. However, shear thinning was stronger with PEEK–AMP filaments at higher frequencies; at 100 rad s^{-1}, the complex viscosity of PEEK–AMP was 10% lesser than PEEK. The increase in complex viscosity at low frequencies can be due to the amplified network formations between the AMP and PEEK particles. Those networks can be destroyed at higher frequencies due to the higher deformation rate reducing the η^* (shear-thinning). In addition, η^* as a function of angular frequency (ω) in the shear thinning regime was fit to a power law model: $\eta^* = k\omega^{n-1}$, where k is the flow consistency index and n is the flow behavior index (Fig. 5(c)). The "n" values were observed to be smaller than 1 (PEEK: 0.08 and PEEK–AMP: 0.12), indicating that PEEK–AMP filaments exhibit shear-thinning properties. Third, AMP addition in PEEK affected the elastic G' and G'' primarily at low frequencies. On the contrary, at higher frequencies, G' and G'' were nearly similar for PEEK and PEEK–AMP [an overlap can be seen in Fig. 5(b)-(ii) and (iii)]. According to the theory of linear viscoelasticity, for homogeneous polymer melts, linear viscoelasticity at low frequencies (terminal zone) reflects fully relaxed polymer chains ($G' \sim \omega^2$ and $G'' \sim \omega$).[40,41] However, for filled polymer systems, G' and G'' can deviate from this behavior.[42]

The viscosity of the filament material is an essential attribute to be considered when they are supposed to be used for 3D printing. The filament material should melt and flow in a controlled manner through the 3D printing nozzle and deposit onto the build plate. In the present case, at low frequencies, PEEK–AMP exhibited higher viscosity. Interestingly, high viscosity in the low-shear region is desirable for 3D printing applications to maintain the shape of the printed layers after deposition.[1,43,44] However, PEEK–AMP filaments exhibit shear thinning and low viscosity at high frequencies. In 3D printing processes, good shear thinning behavior and low viscosity in the high-shear region are expected to smoothen the material flow through the nozzle and improve the coalesce of the molten polymer into solid, uniform 3D printed structures.[45,46] Therefore, rheology analyses of PEEK–AMP filaments indicate a good fit for 3D printing.

3.3 Thermal properties of the PEEK–AMP filaments

The melting temperatures (T_m), enthalpy (H_m), and crystallinity (X_{cw}) are shown in Table 1. The differences in T_m were negligible, but it was evident that T_m and H_m decreased with AMP incorporation in PEEK. On the contrary, PEEK–AMP composites exhibited higher crystallinity than bare PEEK. The increase in crystallinity could be due to AMP crystallization during the extrusion process. For instance, the AMP particles can absorb heat during extrusion and lose the absorbed water molecules, increasing the crystallinity of the overall PEEK–AMP composite. However, as the particles are not exposed to high temperatures for long in the extrusion barrel (as the extrusion process is not prolonged), the AMP particles do not crystallize into a different phase. Moreover, the PEEK matrix acts as a thermal barrier for the AMP particles, resulting in a slight increase in the crystallinity in the PEEK–AMP composite.

Table 1 Thermal properties of PEEK and PEEK–AMP composite filaments

Sample	T_m (°C)	H_m (J g^{-1})	X_{cw} (%) – DSC
PEEK	338.21	32.9869	25.38
PEEK–AMP	339.10	31.3710	25.67

It should be noted that a higher crystallinity is desired for the PEEK-based composites as they can help in obtaining crystalline 3D-printed parts with favorable mechanical properties. Conversely, decreased crystallinity in the feedstock material can reduce the crystallinity of the 3D printed structures, thus affecting the printed part's strength. In addition, amorphous regions in the 3D-printed PEEK-based parts significantly affect the strength of the parts.[1,43,47] Thus, the aim should be to develop crystalline PEEK-based composite feedstock filaments.

3.4 Physical properties of the PEEK–AMP filaments

Fig. 6(a) shows the SEM images of the milled PEEK–AMP powders. The low-magnification SEM images reveal the presence of nano-sized white particles in PEEK. Furthermore, the micrographs indicated that the white particles are homogenously dispersed all over the PEEK particles, confirming a uniform mix of AMP and PEEK particles. In addition, when analyzed closely in the high magnification SEM micrographs, the white particles were seen to be embedded firmly within the PEEK particles. The white particles correspond to the AMP nanoparticles, and it is evident that they are dispersed homogeneously all over the PEEK particles. However, the embedment of the AMP nanoparticles into the PEEK particles resulted in cracks. This is because the high milling speed (400 rpm) forced the AMP particles to embed into PEEK, creating cracks. We can observe the morphology of the AMP nanoparticles embedded in PEEK in some regions. Similar to our previous studies,[19] the AMP particles do not exhibit any specific shape and size, as expected of a typical amorphous material. The particles are in the nanometer range with no distinct geometry.

Fig. 6(b) shows the SEM images of the surface of the PEEK–AMP composite filaments. The AMP particles are seen to be uniformly dispersed on the filament surface; this is primarily beneficial as the AMP particle embedded on the filament surface will help in integrating and interacting with the bone tissues and enhance the bioactivity and osseointegration properties of the composites, as opposed to bare PEEK. Fig. 6(c) shows the SEM images of the cross-sections of the PEEK–AMP composite filaments. The AMP particles are seen to be homogeneously dispersed in the core of the PEEK–AMP filaments, confirming that the milling and the single-screw extrusion helped form the PEEK–AMP composite filaments with a uniform dispersion of the secondary particles in the core of the filaments. Moreover, the corresponding EDS in Fig. 6(a)–(c) reveals the presence of Mg and P, essential elements in

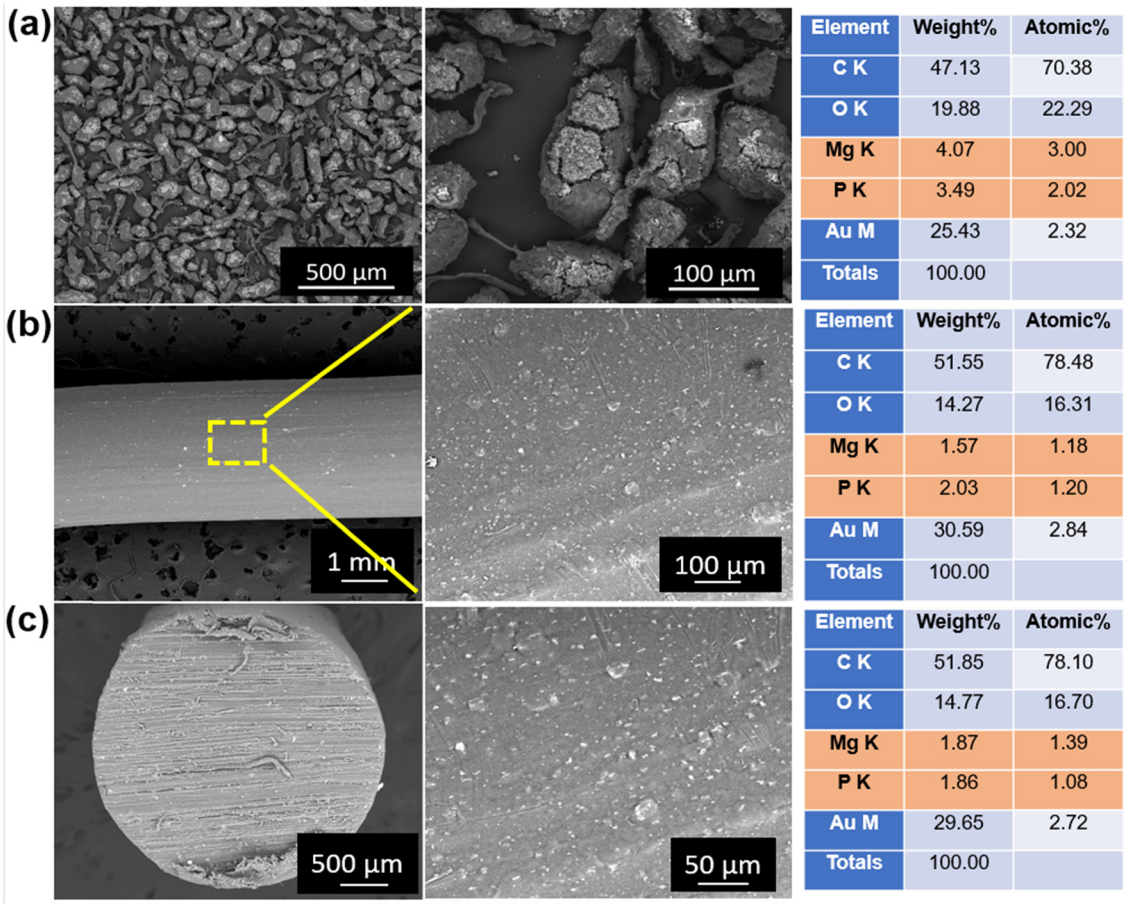

Element	Weight%	Atomic%
C K	47.13	70.38
O K	19.88	22.29
Mg K	4.07	3.00
P K	3.49	2.02
Au M	25.43	2.32
Totals	100.00	

Element	Weight%	Atomic%
C K	51.55	78.48
O K	14.27	16.31
Mg K	1.57	1.18
P K	2.03	1.20
Au M	30.59	2.84
Totals	100.00	

Element	Weight%	Atomic%
C K	51.85	78.10
O K	14.77	16.70
Mg K	1.87	1.39
P K	1.86	1.08
Au M	29.65	2.72
Totals	100.00	

Fig. 6 Scanning electron microscopy of (a) milled PEEK–AMP powders, (b) surfaces, and (c) cross-section of the extruded PEEK–AMP filaments.

AMP, thus confirming the presence of AMP particles in the PEEK matrix.

Homogenous dispersion of the secondary particles in the polymer is essential to achieving the composites' favorable mechanical and material properties. In the present study, 5 vol% AMP did not compromise the dispersion extent of the AMP particles in the PEEK matrix. The amount of secondary particle incorporation plays a significant role in the extent of dispersion. Prior studies have confirmed that a higher content of secondary particles can lead to poor distribution and unwanted agglomerations. Hence, we chose a lower incorporation extent of AMP to ensure the homogenous dispersion. However, we adapted the ball milling process to ensure the mixing of the AMP and PEEK particles before extrusion. We hypothesize that it will also help to uniformly mix higher contents of AMP (such as 15 vol%) in PEEK as a part of follow-up studies. Importantly, solely single-screw extrusion might not be sufficient to disperse the AMP particles in the PEEK matrix. Especially as PEEK has a higher melt viscosity, it is challenging to disperse the bioceramic particles in the PEEK matrix *via* single screw movement. Nevertheless, it might be easier to disperse secondary particles in low-viscosity polymers such as PCL or poly-lactic acid (PLA) with single screw extrusion, as opposed to PEEK.

3.5 Mechanical property analysis

Fig. 7(a) shows the representative stress–strain curves of PEEK and PEEK–AMP parts developed by 3D printing. Notably, the PEEK–AMP composites and PEEK exhibited a mean strength of 89.65 MPa and 89.73 MPa (Table 2), indicating that 5 vol% AMP incorporation did not affect the mechanical strength of the composites. However, Manzoor *et al.* developed PEEK–HA composite filaments with 10 vol% of HA into PEEK matrixes and observed the tensile strength and Young's modulus to be 58.4 MPa and 801.2 MPa, respectively.[48] Fig. 7(b) and (c) provide a comparison of the tensile strengths and Young's modulus of PEEK, PEEK–AMP and PEEK–HA. It is evident that PEEK–AMP exhibits the highest mechanical properties, indicating that 5 vol% AMP incorporation does not decrease the mechanical properties of the composites, instead it increases them slightly as compared to bare PEEK.

Moreover, the SEM analysis of the fractured PEEK–AMP tensile bar surfaces, as shown in Fig. 8 reveal the fracture pattern of the composites. The layers are seen to adhere to each other approvingly, though some interlayer voids can be observed. Interestingly, several varying-sized pores can be seen in the print layers, as indicated by the tallow arrows in Fig. 8. This could be due to the pull-out of AMP particles from the PEEK matrix during fracture.

A spinal fusion cage is a hollow cylinder with walls around used in the treatment for spinal injuries like degenerative disc diseases, spinal instability, and spinal fractures. Generally spinal fusion cages are made with biocompatible materials which help to improve the bone growth formation. We fabricated a robust spinal fusion cage with PEEK–AMP, as shown in Fig. 9, using a fused filament fabrication technique with optimal parameters, shown in Table 4.

Prior studies used various kinds of reinforcements in the PEEK matrix to enhance the mechanical properties of PEEK. For instance, Wang *et al.*[49] developed short carbon fiber (CF) and glass fiber (GF) reinforced high-performance PEEK composite filaments for 3D printing and observed that a lower fiber content of 5 wt% is effective in increasing the mechanical properties, improving surface quality, and reducing the porosity of printed CF/GF–PEEK. Several studies have focused on developing CF-reinforced PEEK (CFR–PEEK), which exhibits enhanced mechanical properties compared with PEEK.[50] However, CF incorporation generally above 12% has resulted in notable degradation in the composite's mechanical properties. On the other hand, secondary particles such as HA have been incorporated in PEEK to enhance the bioactivity properties of PEEK. For Instance, Manzoor *et al.*[48] developed PEEK–HA composite 3D printable filaments and observed no significant differences between the mechanical properties of PEEK–HA and PEEK parts. However, incorporating bioceramic particles in the PEEK matrix, especially in higher contents, has a high chance of notably degrading the mechanical properties of bare PEEK.[51] This might be because the bioceramic particles fail to integrate with the polymer chains and hence do not exhibit a reliable load transfer mechanism from the particles to the matrix. Moreover, bioceramic particles are

Table 2 Mechanical properties of 3D printed PEEK and PEEK–AMP composites

Sample	Tensile strength (MPa ± SD)	Young's modulus (MPa ± SD)	Elongation (% ± SD)
PEEK	89.73 ± 11.24	3325.16 ± 1124.65	2.32 ± 0.35
PEEK–AMP	89.65 ± 10.29	3545.16 ± 1343.85	2.71 ± 0.47
PEEK–HA	58.4 ± 4.5	801.2 ± 72.0	8.8 ± 0.6

Table 3 Extrusion parameters used to form PEEK–AMP filaments

Extrusion parameters	Values
Temperatures	
Heater 1	380 °C
Heater 2	375 °C
Heater 3	370 °C
Heater 4	360 °C
Extrusion rate	6–8 rpm
Cooling rate	60%

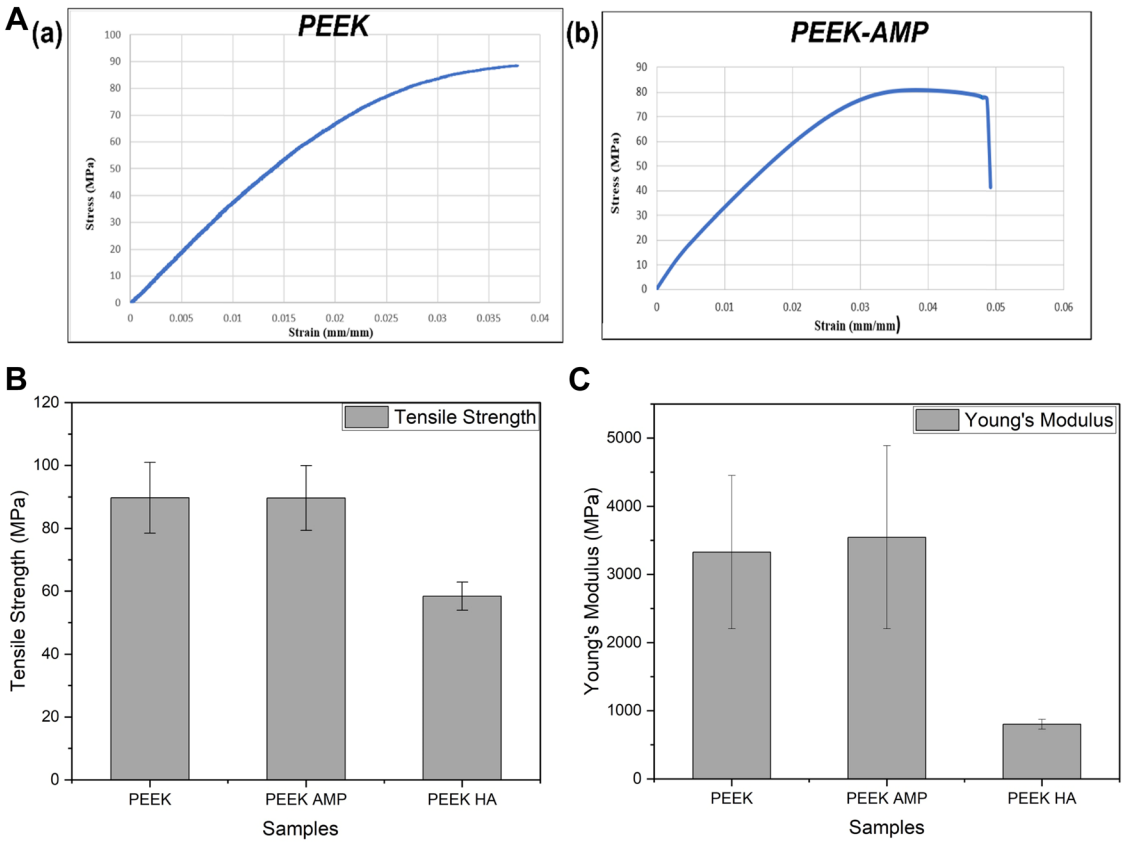

Fig. 7 (a) Representative stress–strain curves of a 3D printed PEEK and PEEK–AMP specimens. Comparison of (b) tensile strength and (c) Young's modulus of PEEK, PEEK–AMP and PEEK–HA.

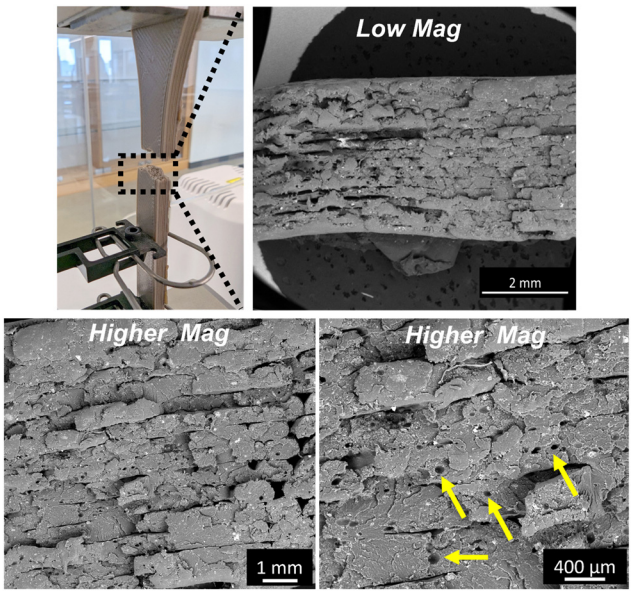

Fig. 8 Scanning electron microscopy (SEM) images of the PEEK–AMP tensile bar fracture surface.

inherently brittle, and excess quantities in the polymer make the composite brittle.

In the present study, 5 vol% AMP bioceramics are used as bioactive particles and do not degrade bare PEEK's mechanical properties. Moreover, the values of the 3D-printed PEEK–AMP specimens are similar to the injection-molded PEEK specimens, denoting that 3D printing can develop parts with comparable mechanical properties to injection-molded ones. The results also confirm that the PEEK–AMP composite filaments are suitable for a FFF setup to develop mechanically durable parts.

In prior studies, we thoroughly analyzed the effect of FFF processing parameters on the material and mechanical properties of the 3D-printed PEEK parts. We observed that thermal parameters, print speed, and layer heights significantly influenced the properties of the printed PEEK parts. In follow-up studies, we will analyze the processing–structure–property relationships of 3D-printed PEEK–AMP composites.

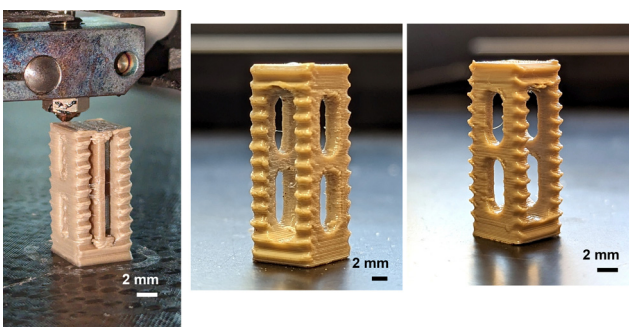

Fig. 9 An ongoing 3D printing of PEEK–AMP spinal fusion cages. Corresponding images show the as-printed PEEK–AMP spinal fusion cages.

Table 4 3D printing parameters used to fabricate spinal fusion cage

3D printing parameters	Values
Nozzle temperature	410 °C
Bedplate temperature	160 °C
Chamber temperature	90 °C
Printing speed	30 mm s^{-1}

4. Conclusion

Extrusion of PEEK to form 3D printable filaments is challenging due to its high melting point, melt-viscosity, and slow polymer crystallization rate. The addition of secondary particles, such as AMP, in the PEEK matrix can interrupt the continuous flow of the polymer and complicate the filament formation process. One of the essential criteria for forming 3D printable filaments is to have a consistent extrusion procedure and provide tension to form uniform-diameter filaments all-throughout. The literature lacks studies focusing on developing 3D printable PEEK or PEEK-based composite filaments. Hence, in this study, we thoroughly investigated the effect of essential extrusion parameters that help form the PEEK-based composite 3D printable filaments. A descending heating gradient with the highest temperature near to the nozzle, moderate screw speed of 6–8 rpm, and cooling rate of 60% were suitable for developing the PEEK–AMP composite filaments. Notably, the filaments were efficiently utilized in a FFF setup to 3D print PEEK–AMP parts with comparable strength to 3D printed and injection molded bare PEEK. The AMP–PEEK filaments developed in this study can potentially disrupt bioinert bare PEEK usage and establish a novel class of composite filaments for bioactive implant manufacturing that can lead to the clinical translation of various customized, multi-functional implants for reconstructive applications in medicine, especially in orthopedics and spinal cases.

Conflicts of interest

There are no conflicts to declare.

Acknowledgements

We are thankful for the STARTUP06 grant at Cleveland State University for this study.

References

1 P. Sikder, B. T. Challa and S. K. Gummadi, A Comprehensive Analysis on the Processing–Structure–Property Relationships of FDM-based 3-D Printed Polyetheretherketone (PEEK) Structures, *Materialia*, 2022, 101427.
2 C. Al Christopher, *et al.*, High performance polymers for oil and gas applications, *React. Funct. Polym.*, 2021, **162**, 104878.
3 S. M. Kurtz, An overview of PEEK biomaterials, *PEEK biomaterials handbook*, 2019, pp. 3–9.

4 W. T. Lee, *et al.*, Stress shielding and fatigue limits of polyether-ether-ketone dental implants, *J. Biomed. Mater. Res., Part B*, 2012, **100**(4), 1044–1052.
5 C. S. Li, *et al.*, The use of carbon-fiber-reinforced (CFR) PEEK material in orthopedic implants: a systematic review, *Clin. Med. Insights: Arthritis Musculoskeletal Disord.*, 2015, **8**, S20354, DOI: 10.4137/CMAMD.S20354.
6 J. M. Toth, *et al.*, Polyetheretherketone as a biomaterial for spinal applications, *Biomaterials*, 2006, **27**(3), 324–334.
7 L. Qin, *et al.*, Review on development and dental applications of polyetheretherketone-based biomaterials and restorations, *Materials*, 2021, **14**(2), 408.
8 S. Singh, *et al.*, Plasma treatment of polyether-ether-ketone: A means of obtaining desirable biomedical characteristics, *Eur. Polym. J.*, 2019, **118**, 561–577.
9 K. Elhattab, *et al.*, Fabrication and evaluation of 3-D printed PEEK scaffolds containing Macropores by design, *Mater. Lett.*, 2020, **263**, 127227.
10 R. Ma, *et al.*, Effects of different sulfonation times and post-treatment methods on the characterization and cytocompatibility of sulfonated PEEK, *J. Biomater. Appl.*, 2020, **35**(3), 342–352.
11 Y. Ren, *et al.*, Microwave assisted coating of bioactive amorphous magnesium phosphate (AMP) on polyether-etherketone (PEEK), *Mater. Sci. Eng., C*, 2018, **85**, 107–113.
12 R. Ma and T. Tang, Current strategies to improve the bioactivity of PEEK, *Int. J. Mol. Sci.*, 2014, **15**(4), 5426–5445.
13 L. L. Koithara, *et al.*, High deposition efficiency and delamination issues during high-pressure cold spraying metallization of PEEK using spherical copper powders, *Int. J. Adv. Manuf. Technol.*, 2020, **107**(11), 4427–4436.
14 F. B. Torstrick, *et al.*, Impaction durability of porous polyether-ether-ketone (PEEK) and titanium-coated PEEK interbody fusion devices, *Spine J.*, 2018, **18**(5), 857–865.
15 J. Dufils, *et al.*, Evaluation of a variety of aC: H coatings on PEEK for biomedical implants, *Surf. Coat. Technol.*, 2017, **313**, 96–106.
16 R. S. Brum, *et al.*, On the sulphonated PEEK for implant dentistry: Biological and physicochemical assessment, *Mater. Chem. Phys.*, 2019, **223**, 542–547.
17 M. Nabiyouni, *et al.*, Magnesium-based bioceramics in orthopedic applications, *Acta Biomater.*, 2018, **66**, 23–43.
18 P. Sikder, *et al.*, Single-phase, antibacterial trimagnesium phosphate hydrate coatings on polyetheretherketone (PEEK) implants by rapid microwave irradiation technique, *ACS Biomater. Sci. Eng.*, 2018, **4**(8), 2767–2783.
19 P. Sikder, *et al.*, Bioactive amorphous magnesium phosphate-polyetheretherketone composite filaments for 3D printing, *Dent. Mater.*, 2020, **36**(7), 865–883.
20 M. Nabiyouni, Y. Ren and S. B. Bhaduri, Magnesium substitution in the structure of orthopedic nanoparticles: A comparison between amorphous magnesium phosphates, calcium magnesium phosphates, and hydroxyapatites, *Mater. Sci. Eng., C*, 2015, **52**, 11–17.
21 K. Elhattab, *et al.*, Fused filament fabrication (three-dimensional printing) of amorphous magnesium phosphate/polylactic acid macroporous biocomposite scaffolds, *ACS Appl. Bio Mater.*, 2021, **4**(4), 3276–3286.
22 N. Dubey, *et al.*, Extracellular matrix/amorphous magnesium phosphate bioink for 3D bioprinting of Craniomaxillofacial bone tissue, *ACS Appl. Mater. Interfaces*, 2020, **12**(21), 23752–23763.
23 P. Sikder, C. R. Grice and S. B. Bhaduri, Processing-structure-property correlations of crystalline antibacterial magnesium phosphate (newberyite) coatings and their in vitro effect, *Surf. Coat. Technol.*, 2019, **374**, 276–290.
24 P. Sikder, Y. Ren and S. B. Bhaduri, Microwave processing of calcium phosphate and magnesium phosphate based orthopedic bioceramics: A state-of-the-art review, *Acta Biomater.*, 2020, **111**, 29–53.
25 H. Zhou, T. J. F. Luchini and S. B. Bhaduri, Microwave assisted synthesis of amorphous magnesium phosphate nanospheres, *J. Mater. Sci.: Mater. Med.*, 2012, **23**(12), 2831–2837.
26 P. Balamurugan and N. Selvakumar, Development of patient specific dental implant using 3D printing, *J. Ambient Intell. Humaniz. Comput.*, 2021, **12**(3), 3549–3558.
27 P.-O. Östman, *et al.*, Clinical outcomes of maxillary anterior postextraction socket implants with immediate provisional restorations using a novel macro-hybrid implant design: An 18-to 24-month single-cohort prospective study, *Int. J. Periodontics Restorative Dent.*, 2020, **40**(3), 355–363.
28 M. F. Huang, *et al.*, The use of patient-specific implants in oral and maxillofacial surgery, *Oral Maxillofac. Surg. Clin.*, 2019, **31**(4), 593–600.
29 D. Rohner, *et al.*, Importance of patient-specific intraoperative guides in complex maxillofacial reconstruction, *J. Craniomaxillofac. Surg.*, 2013, **41**(5), 382–390.
30 S. J. Chu, *et al.*, A Paradigm Change in Macro Implant Concept: Inverted Body-Shift Design for Extraction Sockets in the Esthetic Zone, *Compend. Contin. Educ. Dent.*, 2019, **40**(7), 444–452.
31 M. Al-Sabbagh and A. Kutkut, Immediate implant placement: surgical techniques for prevention and management of complications, *Dent. Clin.*, 2015, **59**(1), 73–95.
32 B. Zhao, *et al.*, Soft tissue integration versus early biofilm formation on different dental implant materials, *Dent. Mater.*, 2014, **30**(7), 716–727.
33 P. Honigmann, *et al.*, Patient-specific surgical implants made of 3D printed PEEK: material, technology, and scope of surgical application, *BioMed Res. Int.*, 2018, **2018**, 4520636.
34 A. Rodrigues and A. Lebugle, Influence of ethanol in the precipitation medium on the composition, structure and reactivity of tricalcium phosphate, *Colloids Surf., A*, 1998, **145**(1–3), 191–204.
35 U. E. Iso, *Plastics-Determination of tensile properties-Part 2: Test conditions for moulding and extrusion plastics*, International Organization for Standardization, Switzerland, 2012.
36 H. Hu, *et al.*, Entrance pressure instability of LLDPE and its composites, *RSC Adv.*, 2016, **6**(85), 81703–81711.

37 F. Wang, *et al.*, Fabrication and characterization of PCL/HA filament as a 3D printing material using thermal extrusion technology for bone tissue engineering, *Polymers*, 2022, **14**(4), 669.
38 P. Geng, *et al.*, Effects of extrusion speed and printing speed on the 3D printing stability of extruded PEEK filament, *J. Manuf. Process.*, 2019, **37**, 266–273.
39 H. Ponsar, R. Wiedey and J. Quodbach, Hot-melt extrusion process fluctuations and their impact on critical quality attributes of filaments and 3D-printed dosage forms, *Pharmaceutics*, 2020, **12**(6), 511.
40 R. M. Ottenbrite, L. A. Utracki and S. Inoue, *Current Topics in Polymer Science: Polymer chemistry and polymer physics*, Munich: Hanser Publishers, Don Mills, Ont., Distributed in Canada by Collier, 1987, vol. 1.
41 K. K. Senanayake, *et al.*, Diffusion of Nanoparticles in Entangled Poly(vinyl alcohol) Solutions and Gels, *Macromolecules*, 2019, **52**(3), 787–795.
42 D. S. Bangarusampath, *et al.*, Rheology and properties of melt-processed poly(ether ether ketone)/multi-wall carbon nanotube composites, *Polymer*, 2009, **50**(24), 5803–5811.
43 B. T. Challa, *et al.*, In-house Processing of 3-D printable Polyetheretherketone (PEEK) filaments and the effect of Fused Deposition Modelling parameters on 3D Printed PEEK structures, *Int. J. Adv. Manuf. Technol.*, 2022, **121**, 1675–1688.
44 S. Y. Sonaye, *et al.*, Patient-specific 3D printed Poly-ether-ether-ketone (PEEK) dental implant system, *J. Mech. Behav. Biomed. Mater.*, 2022, **136**, 105510.
45 N. A. Nguyen, C. C. Bowland and A. K. Naskar, A general method to improve 3D-printability and inter-layer adhesion in lignin-based composites, *Appl. Mater. Today*, 2018, **12**, 138–152.
46 L. G. Blok, *et al.*, An investigation into 3D printing of fibre reinforced thermoplastic composites, *Addit. Manuf.*, 2018, **22**, 176–186.
47 S. Y. Sonaye, *et al.*, Patient-specific 3D Printed Poly-ether-ether-ketone (PEEK) dental implant system, *J. Mech. Behav. Biomed. Mater.*, 2022, 105510.
48 F. Manzoor, *et al.*, 3D printed PEEK/HA composites for bone tissue engineering applications: Effect of material formulation on mechanical performance and bioactive potential, *J. Mech. Behav. Biomed. Mater.*, 2021, **121**, 104601.
49 P. Wang, *et al.*, Preparation of short CF/GF reinforced PEEK composite filaments and their comprehensive properties evaluation for FDM-3D printing, *Composites, Part B*, 2020, **198**, 108175.
50 X. Han, *et al.*, Carbon fiber reinforced PEEK composites based on 3D-printing technology for orthopedic and dental applications, *J. Clin. Med.*, 2019, **8**(2), 240.
51 M. Vaezi, *et al.*, Characterization of new PEEK/HA composites with 3D HA network fabricated by extrusion freeforming, *Molecules*, 2016, **21**(6), 687.